RESEARCH ARTICLE

A Comparative Analysis and Verification of Differentially Expressed miRNAs could Provide New Insights for the Treatment of Endometritis in Yaks

Shuo Wang[1#], Zhipeng Cao[1#], Qingxia Wu[1], Asif Idrees[2], Mikhlid H. Almutairi[3] and Hailong Dong[1*]

[1]Animal Science College, Tibet Agriculture & Animal Husbandry University, Linzhi 860000, China
[2]KBCMA, CVAS, Narowal campus, University of Veterinary and Animal Sciences Lahore 54000, Pakistan
[3]Zoology Department, College of Science, King Saud University, P.O. Box: 2455, 11451, Riyadh, Saudi Arabia
[#]Shuo Wang and Zhipeng Cao contributed equally to this work.
*Corresponding author: 984718586@qq.com

A B S T R A C T

Yak endometritis seriously affects yaks' reproductive performance, causing serious economic problems for the industry. By now, many studies explored the molecular mechanism of endometritis in dairy cows, but limited studies have focused on the regulation of microRNA (miRNA) in yak endometritis. For this reason, the distinguished expressing genes were uncovered by utilizing high-throughput RNA sequencing and validated through quantitative real-time PCR. The findings revealed that uterine epithelial tissue sections from yaks with endometritis had epithelial damage, epithelial bleeding, a high number of inflammatory cell infiltration, and other pathological changes compared to the healthy group. In this study, we identified 114 ($p<0.05$) and 73 ($p<0.01$) clearly different RNAs between the healthy group and the disease group, such as bta-miR-22-3p, bta-miR-96, bta-miR-223, and bta-miR-21-3p. The enrichment analysis of Gene Ontology and Kyoto Encyclopedia of Genes and Genomes revealed that the targeted miRNAs were enriched in different groups, such as cell surface receptor signaling pathway, calcium ion transmembrane transport, adrenergic signaling in cardiomyocytes, protein digestion and absorption, and so on. These results provide a theoretical basis for a deeper understanding of the pathogenesis of yak endometritis, exploring new ideas for specific miRNAs as an effective treatment and diagnosis of yak endometritis, and provides reference significance for the treatment of yak endometritis in the future.

INTRODUCTION

Yak endometritis is an inflammation that occurs in the uterus of yaks 21 days later after parturition (Sheldon *et al.*, 2006). Histologically, yak endometritis was depicted by damage to yak uterine epithelial cells and inflammatory factors (Bondurant, 1999). According to the course of the disease, it could be divided into acute endometritis and chronic endometritis (Kitaya *et al.*, 2018). The symptoms of acute endometritis were placenta retention and lochia in the uterus that could not be excreted, resulting in a large number of bacteria in the uterus, elevated body temperatures in sick animals, mental malaise, loss of appetite, and emotional instability (Brodzki *et al.*, 2015). The symptoms of chronic endometritis were the same as acute endometritis, but the symptoms were more obvious (Kimura *et al.*, 2019). Endometritis has a high incidence and damages the uterus of cattle, which is a great threat to the estrus, reproduction, and postpartum conditions of cattle, and has a certain impact on animal husbandry production (Carneiro *et al.*, 2016a). People were generally treated with antibiotics (Espadamala *et al.*, 2018). However, during treatment, there will be irresponsible use of antibiotics, leading to frequent adverse consequences (Pyörälä *et al.*, 2014). There are also some drugs that can be used instead of antibiotics (Osawa, 2021), but the symptoms are not the root of the disease. So, the research on new treatment methods for endometritis is very urgent.

MiRNA belongs non-coding RNA molecule, which regulates the expression of other genes in eukaryotes and is about 21 to 23 nucleotides long (Umar *et al.*, 2021). Previous studies reported that miRNAs involved in regulating the formation and development of a variety of diseases, such as tumors, inflammation, virus replication,

and so on (Krol *et al.*, 2010). MiRNA uses some base pairs to recognize mRNA and can inhibit its expression (Finnegan and Pasquinelli, 2013). A large part of the protein gene family was controlled by miRNA, so the production of specific miRNA was an important part of gene regulation (Davis-Dusenbery and Hata, 2010). In addition, the biosynthesis and functions of miRNA are strictly and precisely regulated (Treiber *et al.*, 2012). Other people's miRNA research focused on evaluating the regulatory role of miRNA in inflammatory models by in vitro establishing an inflammatory model induced by in vitro establishing an inflammatory model induced by lipopolysaccharide LPS (Ju *et al.*, 2018). MiRNA also has a certain effect on regulation bovine endometritis (Jiang *et al.*, 2020a). However, many studies focus on the molecular mechanism of endometritis in dairy cows. Still, few researches explored the mechanism of miRNA in yak endometritis, resulting in its molecular mechanism being unclear (Lv *et al.*, 2022). We aim to reveal the differentially expressed miRNAs in yak endometritis and to offer a new mentality for the therapy of yak endometritis at the molecular level.

MATERIALS AND METHODS

Sample and treatment: Obtain 3 healthy yak uterine samples from Linzhi Livestock Slaughter Limited Company in Linzhi, Tibet. Additionally, search for 3 yaks with endometritis in Bayi District and Milin County of Linzhi City, Tibet, and collect their uterine samples. Rinse the aforementioned samples thoroughly with PBS buffer solution and preserve the uterine epithelial tissue from the uterine horn in liquid nitrogen. Take several tissue blocks measuring 1.5*1.5cm each from each sample and immerse them in 4% paraformaldehyde fixative solution for preservation. To ensure data accuracy, the entire process should not exceed 4 hours.

Histology and hematoxylin-eosin staining: The collected uterine epithelial tissue samples were fixed in 4% paraformaldehyde solution at room temperature, protected from light, for a minimum of 48 hours. After ethanol dehydration, xylene removal, and paraffin embedding, the tissues were sectioned into 5 μm thick histological slices. Finally, hematoxylin and eosin (HE staining) were performed (Zhang *et al.*, 2017).

Total RNA extraction, Library Construction and High Throughput sequencing: 50 mg of the tissues was collected from the endometrial epithelium of yak. Total RNA was extracted by RNA Easy Fast Tissue/Cell Kit (Tiangen biotech (Beijing) Co., Ltd.). After extracting the total RNA of the sample, it was sent to Bioyi Energy Biotechnology Co., Ltd.,Wuhan, for cDNA library establishment and high-throughput sequencing. Use the library building kit NEBNext Multiplex Small RNA Library Prep Set for Illumina to build the library. After passing the quality inspection, high-throughput sequencing was carried out on the computer.

Processing of sequencing data: The original sequencing data obtained after sequencing will contain joint information, undetected bases (N), and low-quality bases, which will cause great interference with the subsequent information analysis. The interference information will be filtered and removed by fine filtering methods, and the final data will be valid data (Clean reads). The contents of Q20, Q30 and GC were obtained from the effective data. The clean reads obtained were further analyzed.

Quantitative analysis: Based on the results of known sRNA analysis and new sRNA prediction, quantitative analysis counted and normalized the expression of known and new sRNA in every sample using the TPM algorithm. The calculation formula is as follows:

$$\text{Normalized expressions} = \frac{\text{Actual miRNA read count}}{\text{Total count of miRNA reads}} \times 10^6$$

Screening of differentially expressed miRNAs: Bowtie® (v2.2.2), cmsear® (v1.1.2) and chmirdeep2® (v2.0.0.8) were used to compare the miRNAs sequences in the database and predict the new sRNA. If there is no such miRNA in the database, it is a new miRNA. The miRNAs expression data were processed by logarithmic transformation, and the small difference RNA was screened by the R packet (DEseq2). Then the volcanic diagram of differentially expressed miRNAs was drawn by the R packet (DEseq2) "ggplot2".

Prediction and enrichment analysis of differential miRNAs target genes: TargetFinder® and psRobot® (v1.2) were used to predict the target gene and the predicted target genes of miRNAs were analyzed by GO and KEGG.

Quantitative real-time PCR: After RNA extraction from each sample, it was reverse transcribed into cDNA. Then the relative expression of miRNAs was examined by quantitative real-time PCR via $2^{-\Delta\Delta Ct}$ method.

Statistical analysis: The difference between the yak groups was determined using a t-test, and statistical analysis was performed using GraphPad Prism®9 software. The data is presented as mean ± SEM, and a $p < 0.05$ was considered statistically significant.

RESULTS

HE staining: Pathological sections of the disease group show epithelial exfoliation, epithelial bleeding, and many inflammatory cell infiltrations. The result is shown in Fig. 1.

Construction of small RNA Library and High Throughput sequencing: The high-throughput sequencing results revealed a total of $2.09*10^7 \sim 2.64*10^7$ clean reads, encompassing $4.79*10^8 \sim 6.01*10^8$ clean reads base pairs (Table 1).

The results of gene alignment statistics: The comparison results of clean reads showed that D1, D2, D3, H1, H2, H3 had a total of 20857828, 21264789, 26448924, 23823830, 23851302, 25306870, and the matching rates were 98.71%, 98.34%, 98.37%, 97.60%, 98.26%, 98.46%, respectively (Table 2).
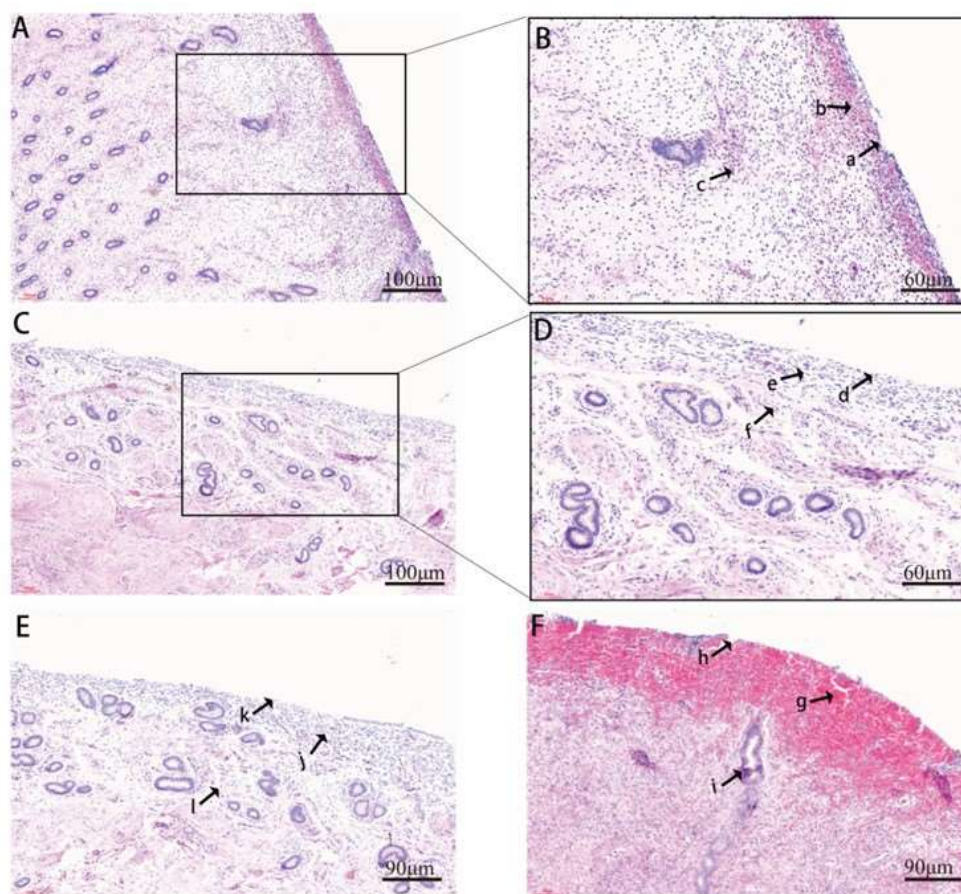
Fig. 1: Histopathological analysis of Uterine Tissue. A: endometrial epithelial tissue section of the disease group (scale: 100 μm). B: Enlargement of diagram A (scale 60 μm). C: endometrial epithelial tissue section of the healthy group (scale: 100 μm). D: Enlargement of diagram C (scale 60 μm). E: endometrial epithelial tissue section of the healthy group (scale: 90 μm). F: endometrial epithelial tissue section of the disease group (scale: 90 μm). Compared with d, a showed epithelial tissue shedding. Compared with e, b showed epithelial tissue bleeding. Compared with f, c showed a high number of inflammatory cell infiltration. Compared with k, h showed epithelial tissue damage. Compared with j, g showed epithelial tissue bleeding. Compared with l, i showed a high number of inflammatory cell infiltration.

Table 1: Statistics of sequencing data volume of each sample.

Sample	total reads	total bases	Q20 rate (%)	Q30 rate (%)	GC (%)
D1	20,857,828	481,945,665	99.09	96.81	43.10
D2	21,264,789	479,139,923	99.35	97.30	43.71
D3	26,448,924	600,978,647	99.45	97.83	44.22
H1	23,823,830	550,065,030	98.63	95.08	45.69
H2	23,851,302	571,708,706	99.05	96.13	46.15
H3	25,306,870	573,853,158	99.02	96.36	45.08

Statistical results and related data of total reads (clean reads number), total bases (clean reads base number), Q20 rate (%) (percentage of base mass value greater than Q20), Q30 rate (%) (percentage of base mass value greater than Q30), GC (%) (percentage of GC content) of each sample.

Table 2: Comparison of SRNA and cattle genome.

Sample name	Total reads	Mapped reads	Percentage (%)
D1	20857828	20589365	98.71
D2	21264789	20911990	98.34
D3	26448924	26018344	98.37
H1	23823830	23251024	97.60
H2	23851302	23436133	98.26
H3	25306870	24917793	98.46

Gene alignment of Total reads (number of reads after data preprocessing and length screening), Mapped reads (number of reads on the reference genome of species) and Percentage (rate of comparison with reference genome) of each sample.

Prediction of miRNAs target genes and results of gene expression and difference analysis: The results showed that RNAhybrid® predicted a total of 25,305 target genes, while miRanda® predicted a total of 16,314 target genes. Additionally, the two software programs jointly predicted 16,314 target genes. (Fig. 2A). Compared with the normal yak endometrial epithelial tissue, the tissue samples with endometritis had significant differential expression. A total of 114 differentially expressed miRNAs (DEGs) were filtered (Fig. 2B), including 65 ($p<0.05$) up-regulated genes and 49 ($p<0.05$) down-regulated genes. Some of the up-regulated and down-regulated gene information is shown in Table 3 and 4.

GO Annotation and KEGG Pathway Analysis: GO is divided into three ontologies, which described the molecular function, cellular component, and biological processes of genes. The result is shown in Fig. 3A. GO enrichment analysis of DEGs implied that in the participating biological process that cell surface receptor signaling pathway, calcium ion transmembrane transport and positive regulation of GTPase activity were the top three aggregates. In the molecular function of the gene, the first three enriched sites were nucleotide binding, guanyl-nucleotide exchange factor activity and ATPase-coupled transmembrane transporter activity. Voltage-gated calcium channel complex and clathrin adaptor complex were enriched cellular components. By using the method of ggplot2 analysis, the scatter diagrams of 20 main GO enrichment quantities of differentially expressed miRNA in samples were drawn (Fig. 3B).

Table 3: partially up-regulated gene information.

Gene-id	Healthy	Disease	log2Fold-Change	P-value	p-adjusted
bta-miR-223	22.99539429	1166.268269	5.6648	$6.8447*10^{-29}$	$4.7982*10^{-26}$
bta-miR-21-3p	225165.615	7059477.596	4.9705	$5.4893*10^{-5}$	$1.5392*10^{-3}$
bta-miR-11983	1.373346938	38.98359208	4.8468	$3.6687*10^{-7}$	$2.2381*10^{-5}$
bta-miR-2284g	0.356606243	10.26758672	4.8265	$1.2088*10^{-2}$	$9.0149*10^{-2}$
bta-miR-12030	0.317880453	8.751609031	4.6038	$1.1686*10^{-3}$	$1.5457*10^{-2}$
bta-miR-206	0.684507997	11.45631631	4.0627	$1.4662*10^{-2}$	$1.0177*10^{-1}$
bta-miR-2285bg	0.660134451	9.568809706	3.8384	$2.9979*10^{-3}$	$3.1841*10^{-2}$
bta-miR-2889	0.698860242	9.198872505	3.7280	$8.6837*10^{-3}$	$7.0782*10^{-2}$
bta-miR-2419-3p	4.45227351	56.72015628	3.6803	$1.8239*10^{-7}$	$1.4206*10^{-5}$
bta-miR-2285bc	0.342253998	4.140852221	3.4817	$3.9989*10^{-2}$	$2.1214*10^{-1}$

These ten genes are most significantly upregulated.

Table 4: partially down-regulated gene information.

Gene-id	Healthy	Disease	log2Fold-Change	P-value	P-adjusted
bta-miR-2474	4.981878345	0.230849297	-3.8782	$1.2694*10^{-2}$	$9.0803*10^{-2}$
bta-miR-22-3p	2679.683934	335.0246604	-3.0000	$9.5863*10^{-6}$	$3.3600*10^{-4}$
bta-miR-96	125.0886007	17.32971446	-2.8579	$5.2631*10^{-3}$	$4.9193*10^{-2}$
bta-miR-184	4.307391649	0.594480343	-2.8268	$4.8652*10^{-2}$	$2.4770*10^{-1}$
bta-miR-148d	632.0940576	114.6922799	-2.4611	$3.9896*10^{-2}$	$2.1214*10^{-1}$
bta-miR-490	562.130408	111.2362896	-2.3354	$9.6684*10^{-3}$	$7.7675*10^{-2}$
bta-miR-29c	387.8697233	77.32126949	-2.3328	$6.7664*10^{-10}$	$9.4865*10^{-8}$
bta-miR-411c-3p	352.9675297	72.45420475	-2.2878	$1.8870*10^{-4}$	$4.4092*10^{-3}$
bta-miR-375	2684.577484	558.8457185	-2.2644	$8.6796*10^{-5}$	$2.2535*10^{-3}$
bta-miR-183	578.3750251	122.4886789	-2.2404	$3.5934*10^{-2}$	$1.9992*10^{-1}$

These are the ten most significantly downregulated genes.
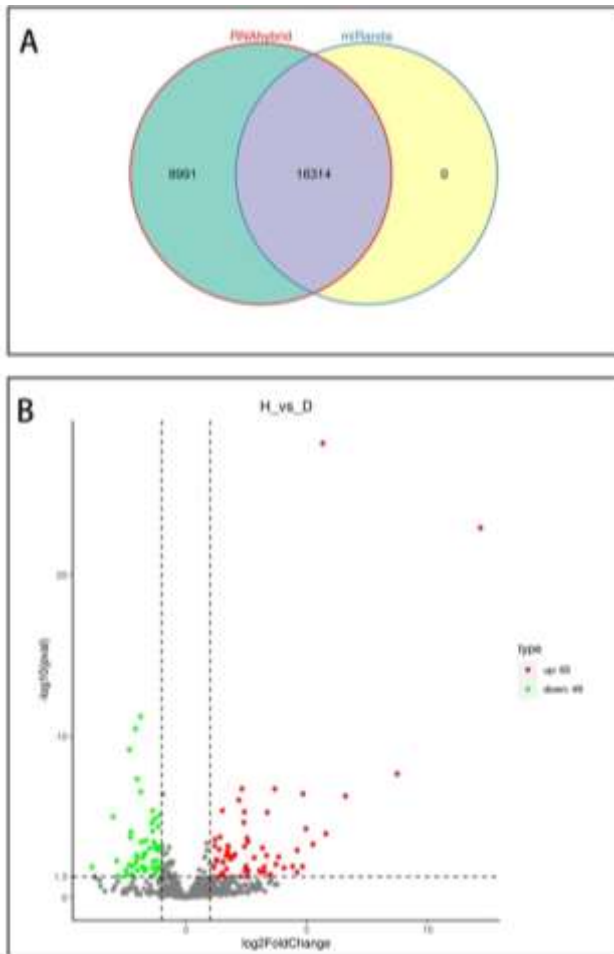
Fig. 2: The differential expression of miRNAs. A: Venn statistical diagram of filtered target gene prediction results. B: DEGs volcano map. (The grey node is the undifferentiated miRNAs; the red node is the up-regulated miRNAs; the green node is the down-regulated miRNAs.)

Pathway enrichment analysis is based on KEGG pathway as a unit, and a hypergeometric test is performed to identify the pathways in which the target genes are appreciably enriched relative to all annotated genes. As shown in Fig. 4A. In this study, using clusterProfiler® software and taking *p-adjust* < 0.05 as the threshold, the significantly enriched KEGG Pathway was found, and the differentially expressed miRNAs were drawn into the reference pathway of KEGG. There were 20 main pathways found in the current study, namely Adrenergic signaling in cardiomyocytes, Aldosterone synthesis and excretion, Longevity regulating pathway, Insulin secretion, Cortisol synthesis and secretion, Regulated calcium reabsorption, Lysine, Valine, leucine and isoleucine degradation, Protein digestion and absorption, beta-Alanine metabolism, cAMP signaling pathway, Glycosaminoglycan biosynthesis- chondroitin sulfate dermatan sulfate, MAPK signaling pathway, Propanoate metabolism, Calcium signaling pathway, ECM-receptor interaction, ABC transporters, cGMP-PKG signaling pathway, Focal adhesion, Lysosome. As shown in Fig. 4B.

Q-PCR: The results revealed significant downregulation of bta-miR-22-3p (*P*<0.01) and significant downregulation of bta-miR-96 (*P*<0.05) in endometritis yaks compared to healthy animals. On the other hand, bta-miR-223 and bta-miR-21-3p exhibited extremely significant upregulation (*P*<0.01), as shown in Fig. 5.

DISCUSSION

Yak endometritis is a common inflammation of the yak endometrium twenty-one days after delivery (Mandhwani *et al.*, 2017). Infection caused by bacteria is the primary cause of endometritis in cattle, while *Escherichia coli* and *Staphylococcus haemolyticus* are the main bacteria (Carneiro *et al.*, 2016b). At present, the treatment of yaks with endometritis with antibiotics is effective, but the abuse of antibiotics is prone to drug resistance (Feldmann *et al.*, 2005). In this study, uterine sections from the disease group showed severe pathological manifestations, including a high number of inflammatory cell infiltration, epithelial bleeding and epithelial cell exfoliation, while in the healthy
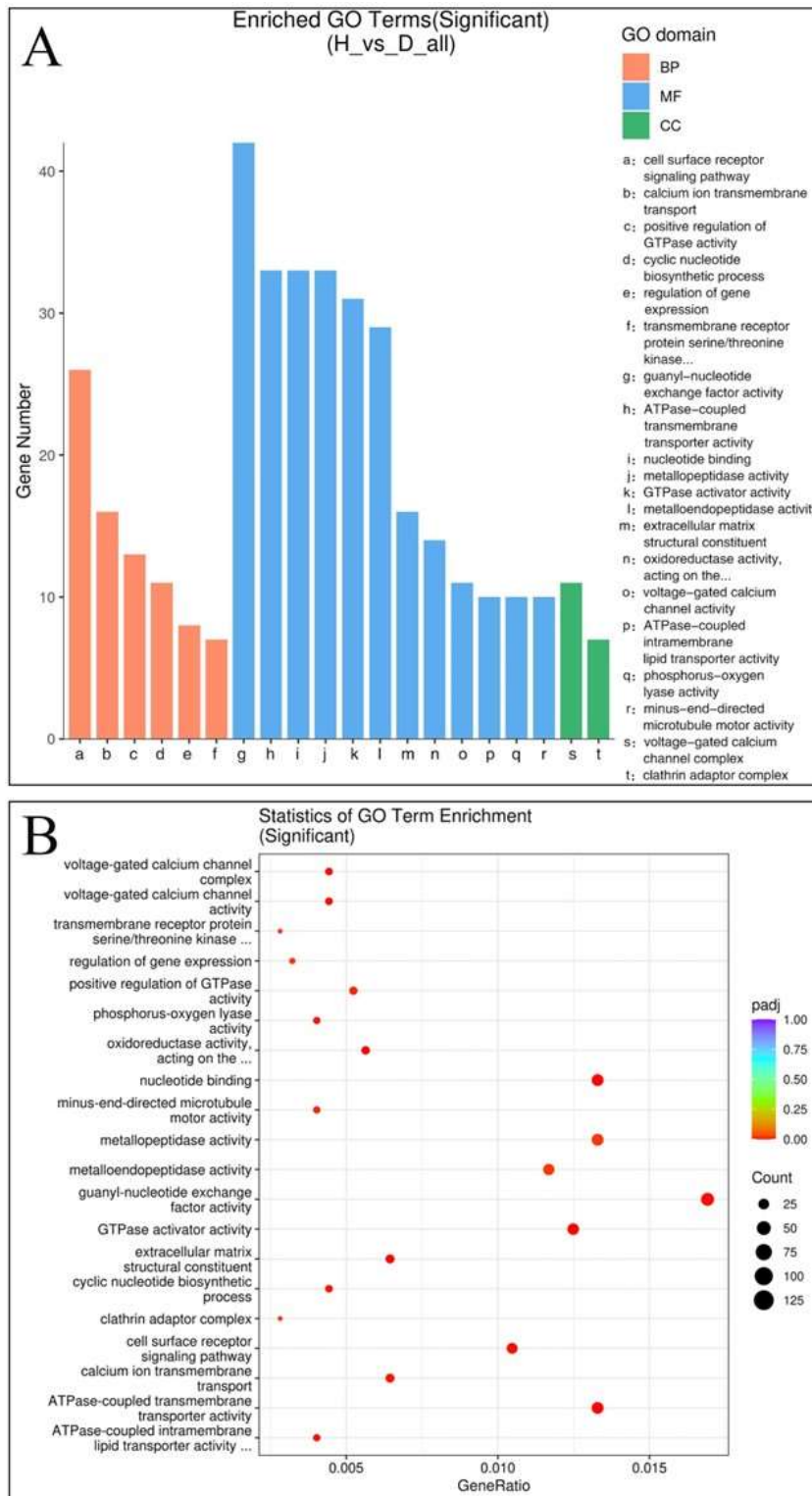
Fig. 3: Go enrichment and classification, annotation, and analysis of differential genes. a: differential gene go enrichment classification histogram; all degs were divided into three categories: molecular function, biological process, and cellular component; differential gene go enrichment histogram, the abscissa is the lower level of go term of three categories of go, and the ordinate is the number of differential genes enriched under the term (including the sub-term of the term). b: the go enrichment and scatter map of differentially expressed miRNA; the abscissa is gene ratio, which indicates the proportion of the number of differentially expressed genes enriched to the total number of differentially expressed genes in the functional annotation results; the ordinate indicates the items on the enrichment; the size of the dot indicates the number of genes on the enrichment, the color indicates the value of *p-adjust*. the lower it is, the more significant it is.

ruminants, limited hyperemia cells were detected and only a few inflammatory cells have been confirmed (Song *et al.*, 2022).

It was found that miR-211 participates in the process of endometritis and contribute to the occurrence of endometritis, which was beneficial to the study of the molecular mechanism of endometritis in its later stages (Yang *et al.*, 2021). Some studies have found that bta-miR-24-3p, miR-643, miR-488, miR-92b, and miR-424-5p acting as important roles in the development of endometritis (Liu *et al.*, 2020; Zhao *et al.*, 2020; Jiang *et al.*, 2021; Oladejo *et al.*, 2021; Umar *et al.*, 2022).

However, the molecular mechanism of miRNA in yak endometritis is still deeply excavated. Based on the current experimental results, we discovered 114 ($P<0.05$) and 73 ($P<0.01$) prominent different genes between the healthy and disease yaks, which can be used to identify target genes to better understand the miRNAs that regulated endometritis in yaks. Previous experiments demonstrated that many miRNAs played significant roles in the process of endometritis. MiR-148a in bovine endometrial epithelial cells induced by lipopolysaccharide was down-regulated compared to control cattle (Jiang *et al.*, 2020b). The overexpression of miR-223 in the inflammatory model in
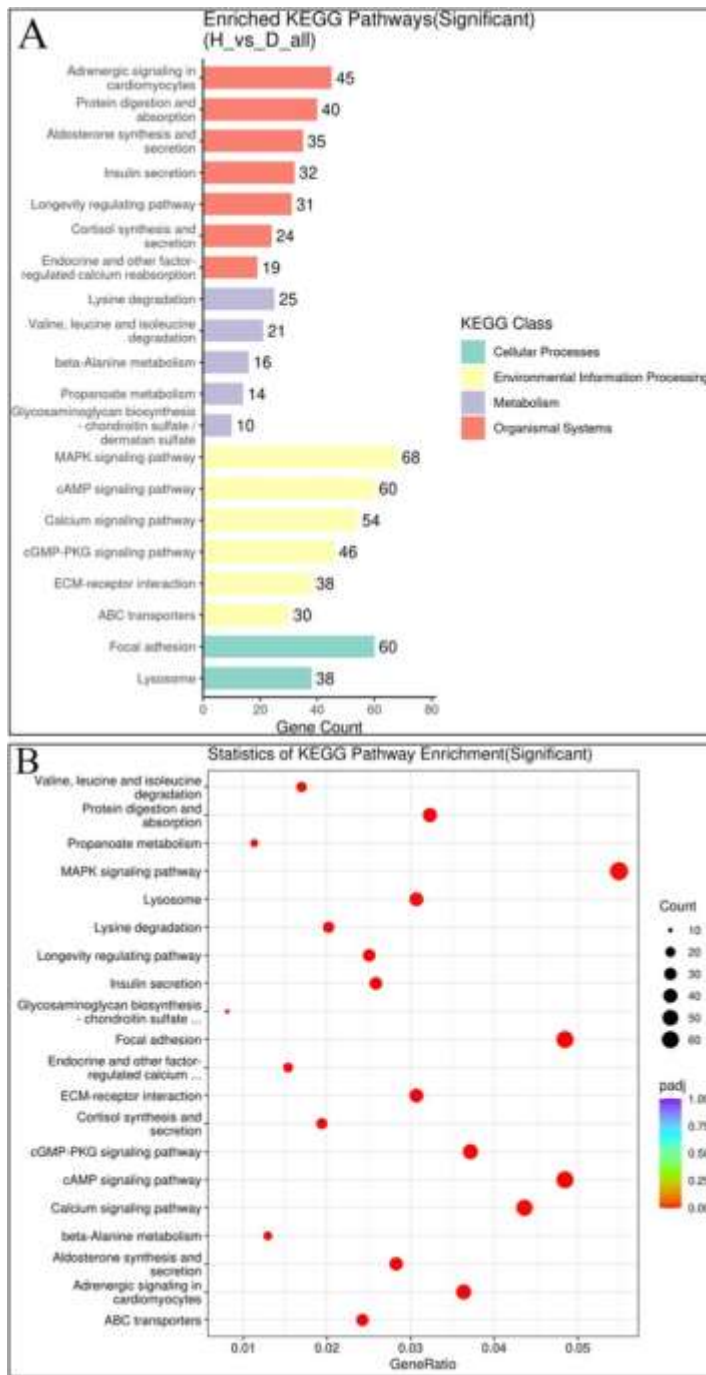
Fig. 4: KEGG enrichment and classification, annotation, and analysis of differential genes. a: KEGG enrichment classification histogram; abscissa is the number of differential genes enriched for the pathway, and ordinate is the KEGG pathway classification. b: KEGG enrichment scatter map; abscissa is gene ratio, indicating the proportion of the number of differential genes enriched for this entry to the total number of differential genes in the functional annotation results; ordinate indicates the items on enrichment; the size of the point implies the number of genes on enrichment, and the lower the value of color indicates the higher significance.
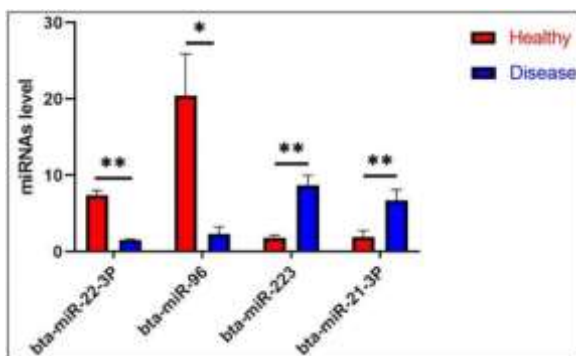
Fig. 5: q-PCR verified the DEGs. The results showed that tsignificant downregulation of bta-miR-22-3p (*P*<0.01) and significant downregulation of bta-miR-96 (*P*<0.05) in endometritis yaks compared to healthy animals.The results showed that bta-miR-223 and bta-miR-21-3p exhibited extremely significant upregulation (*P*<0.01) in the healthy group compared to the disease group.Mean ±SEM,**p < 0.01; * p < 0.05.

vitro could reduce the inflammatory symptoms (Zhao *et al.*, 2018). Furthermore, similar findings holds that Bta-miR-223 negatively regulated inflammatory response (Jiao *et al.*, 2022). In present research, it was found that the expression of bta-miR-223 increased in the disease group, emphasizing the negative regulatory effect on endometritis. At the same time, the KEGG database is a database of pathways, which is extensively applied to estimate the high-order functions of biological systems from its genome information. Our KEGG analysis also showed that the occurrence of endometritis in yaks was primarily related to multiple metabolic pathways, mainly in Adrenergic signaling in cardiomyocytes, Lysine, Aldosterone synthesis and secretion, Insulin secretion, Longevity regulating pathway, Cortisol synthesis and secretion, Vbeta-Alanine metabolism, Propanoate metabolism, Glycosaminoglycan biosynthesis- chondroitin sulfate/

dermatan sulfate, Protein digestion and absorption, ECM-receptor interaction, ABC transporters, regulated calcium reabsorption, aline, leucine and isoleucine degradation, Focal adhesion, Lysosome and so on. It had been previously reported that miRNAs regulating endometritis were related to transferase activity, small molecules binding, MAPK signal pathway, and TNF signal pathway (Yan *et al.*, 2021).These new functional annotations may participated in the regulation of endometritis-related miRNAs. Yet what we know about the molecular mechanism of miRNAs in MAPK signaling pathway is limited, and further study of this annotation pathway will be helpful to understand the pathogenesis of endometritis in yaks.

Conclusions: To sum up, this study screened and verified the differentially expressed miRNAs in yak endometritis, which provided a theoretical basis for further exploration of the pathogenesis of yak endometritis. This study explored new insights into the molecular mechanism of providing a specific miRNA as an effective biomarker for gene diagnosis in yaks.

Ethical approval: All the experiments were performed guided by the Institutional Animal Welfare and Research Ethics Committee of Tibet Agriculture & Animal Husbandry University, China.

Conflicts of interest: The authors declare that they have no competing interests.

Authors contributions: HD and QW provided the research idea. ZC and SW performed the experiments. SW, AI, MHA and ZC wrote the manuscript. SW handled the revision.

REFERENCES

Bondurant RH, 1999. Inflammation in the bovine female reproductive tract. J Anim Sci 77 Suppl 2:101–10.

Brodzki P, Kostro K, Brodzki A, *et al.*, 2015. Inflammatory cytokines and acute-phase proteins concentrations in the peripheral blood and uterus of cows that developed endometritis during early postpartum. Theriogenology 84:11–18.

Carneiro LC, Cronin JG and Sheldon IM, 2016a. Mechanisms linking bacterial infections of the bovine endometrium to disease and infertility. Reprod Biol 16:1–7.

Carneiro LC, Cronin JG and Sheldon IM, 2016b. Mechanisms linking bacterial infections of the bovine endometrium to disease and infertility. Reprod Biol 16:1–7.

Davis-Dusenbery BN and Hata A, 2010. Mechanisms of control of microRNA biogenesis. J Biochem 148:381–92.

Espadamala A, Pereira R, Pallarés P, *et al.*, 2018. Metritis diagnosis and treatment practices in 45 dairy farms in California. J Dairy Sci 101:9608–16.

Feldmann M, Tenhagen Genannt Emming S and Hoedemaker M, 2005. [Treatment of chronic bovine endometritis and factors for treatment success]. Dtsch Tierarztl Wochenschr 112:10–16.

Finnegan EF and Pasquinelli AE, 2013. MicroRNA biogenesis: regulating the regulators. Crit Rev Biochem Mol Biol 48:51–68.

Jiang K, Yang J, Yang C, *et al.*, 2020a. miR-148a suppresses inflammation in lipopolysaccharide-induced endometritis. J Cell Mol Med 24:405–17.

Jiang K, Yang J, Song C, *et al.*, 2021. Enforced expression of miR-92b blunts E. coli lipopolysaccharide-mediated inflammatory injury by activating the PI3K/AKT/β-catenin pathway via targeting PTEN. Int J Biol Sci 17:1289–1301.

Jiao P, Wang J, Yang J, *et al.*, 2022. Bta-miR-223 Targeting the RHOB Gene in Dairy Cows Attenuates LPS-Induced Inflammatory Responses in Mammary Epithelial Cells. Cells 11:3144.

Ju M, Liu B, He H, *et al.*, 2018. MicroRNA-27a alleviates LPS-induced acute lung injury in mice via inhibiting inflammation and apoptosis through modulating TLR4/MyD88/NF-κB pathway. Cell Cycle 17:2001–18.

Kimura F, Takebayashi A, Ishida M, *et al.*, 2019. Review: Chronic endometritis and its effect on reproduction. J Obstet Gynaecol Res 45:951–60.

Kitaya K, Takeuchi T, Mizuta S, *et al.*, 2018. Endometritis: new time, new concepts. Fertil Steril 110:344–50.

Krol J, Loedige I and Filipowicz W, 2010. The widespread regulation of microRNA biogenesis, function and decay. Nat Rev Genet 11:597–610.

Liu J, Guo S, Jiang K, *et al.*, 2020. miR-488 mediates negative regulation of the AKT/NF-κB pathway by targeting Rac1 in LPS-induced inflammation. J Cell Physiol 235:4766–77.

Lv C, Li Z, Wang Q, *et al.*, 2022. miRNA-150_R-1 mediates the HIF-1/ErbB signaling pathway to regulate the adhesion of endometrial epithelial cells in cows experiencing retained placenta. Front Vet Sci 9:1037880.

Mandhwani R, Bhardwaz A, Kumar S, *et al.*, 2017. Insights into bovine endometritis with special reference to phytotherapy. Vet World 10:1529–1532.

Oladejo AO, Li Y, Shen W, *et al.*, 2021. MicroRNA Bta-miR-24-3p Suppressed Galectin-9 Expression through TLR4/NF-κB Signaling Pathway in LPS-Stimulated Bovine Endometrial Epithelial Cells. Cells 10:3299.

Osawa T, 2021. Predisposing factors, diagnostic and therapeutic aspects of persistent endometritis in postpartum cows. J Reprod Dev 67:291–99.

Pyörälä S, Taponen J and Katila T, 2014. Use of antimicrobials in the treatment of reproductive diseases in cattle and horses. Reprod Domest Anim 49 Suppl 3:16–26.

Sheldon IM, Lewis GS, LeBlanc S, *et al.*, 2006. Defining postpartum uterine disease in cattle. Theriogenology 65:1516–30.

Song P, Liu C, Sun M, *et al.*, 2022. Oxidative Stress Induces Bovine Endometrial Epithelial Cell Damage through Mitochondria-Dependent Pathways. Animals (Basel) 12:2444.

Treiber T, Treiber N and Meister G, 2012. Regulation of microRNA biogenesis and function. Thromb Haemost 107:605–10.

Umar T, Yin B, Umer S, *et al.*, 2021. MicroRNA: Could It Play a Role in Bovine Endometritis? Inflammation 44:1683–95.

Umar T, Ma X, Yin B, *et al.*, 2022. miR-424-5p overexpression inhibits LPS-stimulated inflammatory response in bovine endometrial epithelial cells by targeting IRAK2. J Reprod Immunol 150:103471.

Yan C, Lv H, Peng Z, *et al.*, 2021. Analysis of miRNA expression changes in bovine endometrial stromal cells treated with lipopolysaccharide. Theriogenology 167:85–93.

Yang C, Yang C, Zhang J, *et al.*, 2021. MicroRNA-211 regulates the expression of TAB1 and inhibits the NF-κB signaling pathway in lipopolysaccharide-induced endometritis. Int Immunopharmacol 96:107668.

Zhang H, Wang Y, Li K, *et al.*, 2017. Sero-prevalence and Pathological Examination of Lymphoid Leukosis Virus Subgroup A in Chickens in Anhui Province, China. Pakistan Journal of Zoology 49:1033–37.

Zhao G, Jiang K, Yang Y, *et al.*, 2018. The Potential Therapeutic Role of miR-223 in Bovine Endometritis by Targeting the NLRP3 Inflammasome. Front Immunol 9:1916.

Zhao R, Wang J, Zhang X, *et al.*, 2020. MiR-643 inhibits lipopolysaccharide-induced endometritis progression by targeting TRAF6. Cell Biol Int 44:1059–67.